THE JOURNAL OF BIOLOGICAL CHEMISTRY VOL. 284, NO. 19, pp. 13077–13085, May 8, 2009

Dendritic Assembly of Heteromeric γ-Aminobutyric Acid Type B Receptor Subunits in Hippocampal Neurons[S]

Received for publication, January 27, 2009, and in revised form, March 9, 2009 Published, JBC Papers in Press, March 10, 2009, DOI 10.1074/jbc. M900575200

Omar A. Ramírez[‡1], René L. Vidal[‡§2], Judith A. Tello[‡], Karina J. Vargas[‡§], Stefan Kindler[¶3], Steffen Härtel[‖4], and Andrés Couve[‡**5]**

*From [‡]Physiology and Biophysics, Faculty of Medicine, Universidad de Chile, Independencia 1027, Santiago 8380000, Chile, [‖]Anatomy and Development and the **Nucleus of Neural Morphogenesis, Faculty of Medicine, Universidad de Chile, Santiago 8380000, Chile, the [¶]Institut fuer Humangenetik, Universitaetsklinikum Hamburg-Eppendorf, D-20246 Hamburg, Germany, and the [§]Universidad Austral de Chile, Valdivia 5090000, Chile*

Understanding the mechanisms that control synaptic efficacy through the availability of neurotransmitter receptors depends on uncovering their specific intracellular trafficking routes. γ-Aminobutyric acid type B ($GABA_B$) receptors ($GABA_B$Rs) are obligatory heteromers present at dendritic excitatory and inhibitory postsynaptic sites. It is unknown whether synthesis and assembly of $GABA_B$Rs occur in the somatic endoplasmic reticulum (ER) followed by vesicular transport to dendrites or whether somatic synthesis is followed by independent transport of the subunits for assembly and ER export throughout the somatodendritic compartment. To discriminate between these possibilities we studied the association of $GABA_B$R subunits in dendrites of hippocampal neurons combining live fluorescence microscopy, biochemistry, quantitative colocalization, and bimolecular fluorescent complementation. We demonstrate that $GABA_B$R subunits are segregated and differentially mobile in dendritic intracellular compartments and that a high proportion of non-associated intracellular subunits exist in the brain. Assembled heteromers are preferentially located at the plasma membrane, but blockade of ER exit results in their intracellular accumulation in the cell body and dendrites. We propose that $GABA_B$R subunits assemble in the ER and are exported from the ER throughout the neuron prior to insertion at the plasma membrane. Our results are consistent with a bulk flow of segregated subunits through the ER and rule out a post-Golgi vesicular transport of preassembled $GABA_B$Rs.

The efficacy of synaptic transmission depends on the intracellular trafficking of neurotransmitter receptors (1, 2). The trafficking of glutamatergic and $GABA_A$[6] receptors has been extensively studied, and their implications for synaptic plasticity have been well documented (3, 4). For example, differential trafficking of α-amino-3-hydroxy-5-methyl-4-isoxazolepropionic acid (AMPA) receptors modifies synaptic strength and influences experience-dependent plasticity *in vivo* (5). The molecular mechanisms that govern the trafficking of metabotropic $GABA_B$Rs and their consequences for synaptic inhibition remain less clear. In particular, limited information is available regarding the relationship between the trafficking of $GABA_B$Rs and the topological complexity of the secretory pathway in neurons.

$GABA_B$Rs mediate the slow component of synaptic inhibition by acting on pre- and postsynaptic targets (6–8). They are implicated in epilepsy, anxiety, stress, sleep disorders, nociception, depression, and cognition (9). They also represent attractive targets for the treatment of withdrawal symptoms from drugs of addiction such as cocaine (10). They are obligatory heteromers composed of $GABA_B$R1 and $GABA_B$R2 subunits. $GABA_B$R1 contains an *RXR*-type sequence in the intracellular C-terminal domain that functions as an ER retention motif (11, 12). The ER retention sequence is masked upon assembly with $GABA_B$R2 resulting in the appearance of functional receptors at the plasma membrane. Only $GABA_B$R1 binds GABA with high affinity, whereas G protein signaling is exclusively mediated by the second and third intracellular loops of $GABA_B$R2 (13–15). $GABA_B$Rs are located in dendrites and axons, but their distribution does not coincide with the active zone or the postsynaptic density. Rather, they are adjacent to both compartments constituting perisynaptic receptors (16, 17).

If $GABA_B$R subunits are synthesized in the soma, at least two possibilities exist for their anterograde transport, assembly, and insertion in dendrites. First, the subunits may be synthesized in

[S] The on-line version of this article (available at http://www.jbc.org) contains supplemental Figs. S1–S4.

[1] Supported by Mejoramiento de la Calidad y Equidad de la Educación Superior (MECESUP).
[2] Supported by Comisión Nacional de Investigación Científica y Tecnológica (CONICYT).
[3] Supported by Grants Ki488/2-6 and KR 1321/4-1.
[4] Supported by Fondo Nacional de Desanollo Cientifico y Tecnologico (FONDECYT) Grant 1060890.
[5] Supported by FONDECYT Grant 1071001, Iniciativa Científico Milenio (ICM) Grant P07-048-F, Human Frontiers Science Program Organization (HFSPO) Grant ST00105/2005-C, and Deutsche Forschungsgemeinschaft Forschergruppe 885. To whom correspondence should be addressed: Programa de Fisiología y Biofísica, Instituto de Ciencias Biomédicas (ICBM), Facultad de Medicina, Universidad de Chile, Independencia 1027, Santiago, Chile. Tel.: 56-2-978-6878; Fax: 56-2-777-6916; E-mail: andres@neuro.med.uchile.cl.

[6] The abbreviations used are: $GABA_A$, γ-aminobutyric acid, type A; $GABA_B$R, GABA type B receptor; AMPA, α-amino-3-hydroxy-5-methyl-4-isoxazolepropionic acid; GluR, glutamate receptor; C/EBP, CAAT/enhancer-binding protein; GM130, *cis*-Golgi matrix protein; ER, endoplasmic reticulum; TGN, *trans*-Golgi network; PM, near the plasma membrane of a dendrite; CR, core region of a dendrite; DIV, days *in vitro*; FRAP, fluorescence recovery after photobleaching; BiFC, bimolecular fluorescent complementation; $GABA_B$R-BiFC, $GABA_B$R-dependent BiFC; FISH, fluorescence *in situ* hybridization; M_1 or M_2, Manders coefficients 1 or 2; ROIs, regions of interest; EGFP, enhanced green fluorescent protein; mRFP, monomeric red fluorescent protein; YFP, yellow fluorescent protein; BFA, brefeldin A; HA, influenza A virus epitope; TRITC, tetramethyl rhodamine isothiocyanate; Cy3, cyanine.

the cell body, assembled in the somatic ER, and targeted preassembled in post-Golgi vesicles to their site of insertion in dendrites. Alternatively, they may be synthesized in the soma and transported through the ER membrane as non-heteromeric subunits. In the latter scenario, newly assembled receptors may exit the ER throughout the somatodendritic compartment prior to insertion at the plasma membrane and diffuse laterally for retention at functional sites. No evidence exists to discriminate between these possibilities. We reasoned that a prevalence of associated subunits in post-Golgi vesicles in dendrites would favor the first alternative, whereas the existence of non-associated subunits in intracellular compartments would support a somatodendritic assembly mechanism. Here we explore the presence of associated GABA$_B$R subunits using fluorescence recovery after photobleaching (FRAP), biochemistry, and quantitative colocalization. In addition, we report for the first time the use of BiFC (18) to study GABA$_B$R assembly in neurons. Our results demonstrate that GABA$_B$R subunits are differentially mobile in dendrites and that a high proportion of non-associated subunits prevail in an intracellular fraction of the adult brain. They also show that GABA$_B$R subunits are heteromeric at the plasma membrane but segregated in intracellular compartments of dendrites of hippocampal neurons. Importantly, treatment with brefeldin A (BFA) or interference of the coatomer protein complex II impair ER export and result in the accumulation of assembled subunits in intracellular compartments throughout the somatodendritic arbor. We conclude that GABA$_B$R subunits are synthesized in the soma and remain segregated in intracellular compartments prior to somatodendritic assembly. Our observations rule out a post-Golgi vesicular transport of preassembled GABA$_B$Rs and suggest an alternative mechanism of receptor targeting.

EXPERIMENTAL PROCEDURES

Animals—Adult pregnant female Sprague-Dawley rats were purchased from the Central Animal Facility at Universidad Católica de Chile and killed by asphyxia in a CO_2 chamber according to the Guide for Care and Use of Laboratory Animals (National Academy of Sciences, 1996).

Cell Lines, Neuronal Cultures, and Transfection—COS-7 cells were maintained and transfected as described previously using a GenePulser Xcell (Bio-Rad) (11). Primary hippocampal neurons were cultured from E18 rats and transfected by using Ca^{2+} phosphate (19, 20). Endogenous subunits interfere in the assembly of recombinant subunits only after 4–5 days post-transfection; therefore, all experiments were analyzed between 48 and 72 h post-transfection.

DNA Constructs—Myc-GABA$_B$R1, HA-GABA$_B$R2, Myc-GABA$_B$R1$_{ASA}$, and HA-GABA$_B$R2$_{R1C}$ have been described and contain epitope tags on the extracellular N-terminal domains (11, 21–23). GABA$_B$R1a-enhanced green fluorescent protein (EGFP) was generated by subcloning the SpeI/PstI fragment of rat GABA$_B$R1a into pEGFP-N1 (Clontech, Mountain View, CA) and adding the extreme C-terminal sequence amplified by PCR to provide an in-frame fusion at the C terminus (primers: forward, 5′-GCCTGCAGCTCCAAGAAGATGAATACG-TGG-3′; reverse, 5′-GCCTGCAGCTTGTAAAGCAAATGTA-CTCG-3′). GABA$_B$R1a-monomeric red fluorescent protein (mRFP) was generated by subcloning the SpeI/BamHI fragment of rat GABA$_B$R1a into a modified version of pEGFP-N1 containing mRFP and subsequently adding the BamHI fragment from GABA$_B$R1a-EGFP containing the extreme C-terminal sequence of GABA$_B$R1a to provide an in-frame fusion at the C terminus. GABA$_B$R2-EGFP was generated by PCR amplification of rat GABA$_B$R2 (primers: forward, 5′-GCGAATTCA-TGGCTTCCCCGCCGAGCTC-3′; reverse, 5′-GCGGTACC-AGGCCCGAGACCATGACTC-3′) and subcloned into pEGFP-N1 (Clontech). GABA$_B$R1-N-yellow fluorescent protein (YFP) and GABA$_B$R2-C-YFP were generated into N-YFP-pcDNA3.1 and C-YFP-pcDNA3.1 kindly provided by F. Ciruela (University of Barcelona). GABA$_B$R1-N-YFP was generated by cloning an EcoRV fragment containing GABA$_B$R1 into N-YFP-pcDNA3.1 and replacing the 3′ region to obtain an in-frame fusion at the C terminus using BstEII/XhoI (primers: forward, 5′-GCGGTTACCACATTGGGAGG-3′; reverse, 5′-GCC-TCGAGCTTATAAAGCAAATGCAC-3′). GABA$_B$R2-C-YFP was generated by subcloning a HindIII/EcoRV fragment containing the 5′ of GABA$_B$R2 into C-YFP-pcDNA3.1 and completing the 3′ in-frame using EcoRV/XhoI (primers: forward, 5′-GCGATAT-CTCCATCCGCCCTC-3′; reverse, 5′-GCCTCGAGCAGGCC-CGAGACCATGAC-3′). All manipulations and fidelity of DNA constructs were verified by sequencing.

Antibodies—Chicken GABA$_B$R1 antibodies (which recognize GABA$_B$R1a and GABA$_B$R1b) and GABA$_B$R2 antibodies against intracellular C-terminal domains were provided by S. J. Moss (Tufts University) and have been characterized previously (24). Guinea pig GABA$_B$R1 (which recognize GABA$_B$R1a and GABA$_B$R1b), GABA$_B$R2, and microtubule-associated protein 2 antibodies were purchased from Chemicon (Temecula, CA). Piccolo and Bassoon antibodies were provided by E. D. Gundelfinger and W. D. Altrock (Leibniz Institute for Neurobiology, Magdeburg, Germany). Glutamate receptor (GluR) 2, *cis*-Golgi matrix protein 130 (GM130), and calnexin antibodies were purchased from BD Biosciences (San Jose, CA). KDEL antibodies (Grp78 and BiP) were purchased from Stressgen (Ann Arbor, MI). Myc antibodies were purchased from Sigma. Influenza A virus epitope (HA) antibodies were purchased from Roche Applied Science. Secondary anti-mouse, anti-rabbit, anti-guinea pig, or anti-chicken antibodies conjugated to Texas Red, tetramethyl rhodamine isothiocyanate (TRITC), fluorescein isothiocyanate, or cyanine (Cy3) were purchased from Jackson ImmunoResearch Laboratories (West Grove, PA).

Immunofluorescence, Cell Fractionation, and Immunoprecipitation—These methodologies were performed as described previously (25, 26).

Fluorescence in Situ Hybridization—FISH was performed as reported previously (27). Antisense probes for GABA$_B$R subunits were generated by PCR amplification of rat GABA$_B$R1a (2243 bp, 5′-CTACGAGCTCAAGCTTATCCAC-3′ and 5′-CTCGACTCCCATCACAGCTAAG-3′) and GABA$_B$R2 (2453 bp, 5′-CTGGACCTGCGACTCTATGAC-3′ and 5′-CTGAC-GCAGCTGGCATCCAC-3′) and subcloned into pGEM-T-Easy (Promega, Madison, WI).

Image Capture, Colocalization, FRAP, and Time-lapse Microscopy—For colocalization and FRAP, confocal image stacks were captured with a Zeiss LSM-5, Pascal 5 Axiovert 200M microscope, using LSM 5 3.2 image capture and analysis software and a Plan-Apochromat 63×/1.4 oil differential interference contrast objective. An approach based on Costes *et al.*, using Manders coefficients (M_1 or M_2) was used to measure colocalization (28, 29). All parameters were kept constant for a particular type of experiment (*e.g.* native $GABA_BR1$ and $GABA_BR2$ in dendrites). Images were acquired in 8 bits. Two-channel fluorescent image stacks (intensity, $I(x,y,z) \in [0, 255]$; voxel size, $\Delta x/\Delta y/\Delta z = 70/70/300$ nm) were recorded in the multitrack mode. Channel-1 (fluorescein isothiocyanate) had an excitation/emission wavelength of $\lambda_{exc}/\lambda_{em} = 488/505–530$ nm, and channel-2 (Texas Red/TRITC) had an excitation/emission wavelength of with $\lambda_{exc}/\lambda_{em} = 543/>560$ nm. We guaranteed that $I(x,y,z)$ did not saturate and that image background was slightly above zero by carefully adjusting the laser power, detector gain, and detector offset. Digital zoom (4×), rotation (none), and lines (four) were kept constant. In the multitrack mode, a spatial shift in the focal *x-y* plane was observed, probably due to mechanical factors such as the repositioning of the scanners. We calibrated the *x-y* shift with a grid and corrected all images before the calculation of colocalization coefficients. Raw confocal image stacks were deconvolved by Huygens Scripting software (Scientific Volume Imaging, Hilversum, Netherlands) using an algorithm based on the classic maximum likelihood estimator. Deconvolution improves the signal-to-noise ratio and is essential for a reliable analysis of colocalization coefficients. Image-processing routines were developed in our laboratory based on of Interactive Data Language (ITT, Boulder, CO), including routines for segmentation of different regions of interest (ROIs), visualization, calculation of colocalization coefficients, and statistical validation of the colocalization coefficients.

Reliable segmentation of ROIs in neuronal projections was achieved by applying gradient filters and selecting threshold values in the gradient histograms, which resulted in a homogeneous definition of the borders of receptor signals. Remaining holes inside receptor signals and segmented signals outside defined neuronal projections were filled or removed by morphological filters. The quality of the segmentation was controlled interactively by overlaying the original fluorescent images with the mask in each channel. Importantly, the segmentation criterion was kept constant for all images within a particular category (*e.g.* "dendrites").

For the quantification of colocalization we calculated M_1 and M_2 between ROIs 1 and 2, by the following definition,

$$M_1 = \frac{\sum_i I_{Ch1(ROI1 \cap ROI2)}}{\sum_i I_{Ch1(ROI1)}}, \quad M_2 = \frac{\sum_i I_{Ch2(ROI1 \cap ROI2)}}{\sum_i I_{Ch2(ROI2)}} \qquad \text{(Eq. 1)}$$

where M_1 and M_2 sum up the contribution of the respective fluorescence intensities in the colocalizing region $I_{Ch1/2}(ROI1 \cap ROI2)$ and divide the number by the sum of the fluorescence intensities $I_{Ch1/Ch2}$ inside of the segmented regions $I_{Ch1}(ROI1)$ or $I_{Ch2}(ROI2)$. ROI1 and ROI2 are segmented as described above and not by setting $I(x,y,z)$ above zero in the respective fluorescent channels. M_1 and M_2 can be understood as the amount of colocalizing signal relative to the total amount of segmented signal.

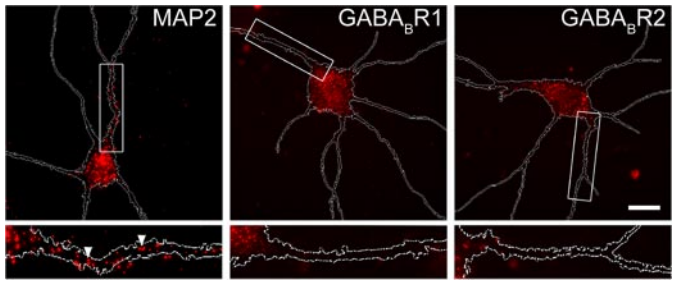

FIGURE 1. **The mRNAs for $GABA_BR$ subunits are concentrated in the neuronal soma.** Rat hippocampal neurons grown in culture were fixed at 14 DIV and processed for FISH with digoxigenin-labeled antisense probes to microtubule-associated protein 2 or the $GABA_BR$ subunits. The probes were detected using digoxigenin and secondary antibodies conjugated to Cy3. The outline of each neuron is drawn in *white*. *Lower panels* correspond to high magnification images of *boxed areas* above.

FRAP experiments were performed at ambient temperature in a 23 °C equilibrated microscopy suite as described previously (25). Dendritic ROIs of 100 μm^2, 15 μm away from the soma, were bleached for 8 s with the argon 488 nm laser at 100% power. The fluorescence recovery was measured every 10 s at 5% laser power by imaging the entire field. Boxes of 9 μm^2 were selected within the original photobleached ROI to quantify recovery using ImageJ. For time-lapse microscopy, images were obtained using an Olympus BX61WI upright microscope and an Olympus disk-scanning unit. Consecutive frames were acquired every 30 s over a period of 30 min.

RESULTS

$GABA_BR$ Subunits Are Transported to Dendrites and Display Differential Mobility—To define the intracellular trafficking route used by $GABA_BR$ subunits we determined whether dendritic anterograde transport operated on protein subunits or whether mRNA targeting contributed to receptor localization. To discriminate between these possibilities the subcellular localization of $GABA_BR$ mRNAs in hippocampal neurons was examined via FISH. Importantly, both mRNAs concentrated in the somatic region and were absent from dendrites (Fig. 1). On the contrary, the mRNA for microtubule-associated protein 2, an established marker for dendritic mRNA, accumulated in distal dendrites (Fig. 1, *arrowheads*). This evidence agrees with previous studies (13, 30) and suggests that $GABA_BR$ subunits are synthesized in the cell body and transported to dendrites via the secretory pathway.

We visualized the mobility of the subunits in live hippocampal neurons by FRAP using $GABA_BR1$ and $GABA_BR2$ fused to EGFP. Importantly, both EGFP-fused subunits maintained their trafficking properties relative to native subunits and efficiently coupled to G-protein inwardly rectifying potassium channels (supplemental Fig. S1 and data not shown). In dendrites $GABA_BR1$-EGFP did not reach the plasma membrane

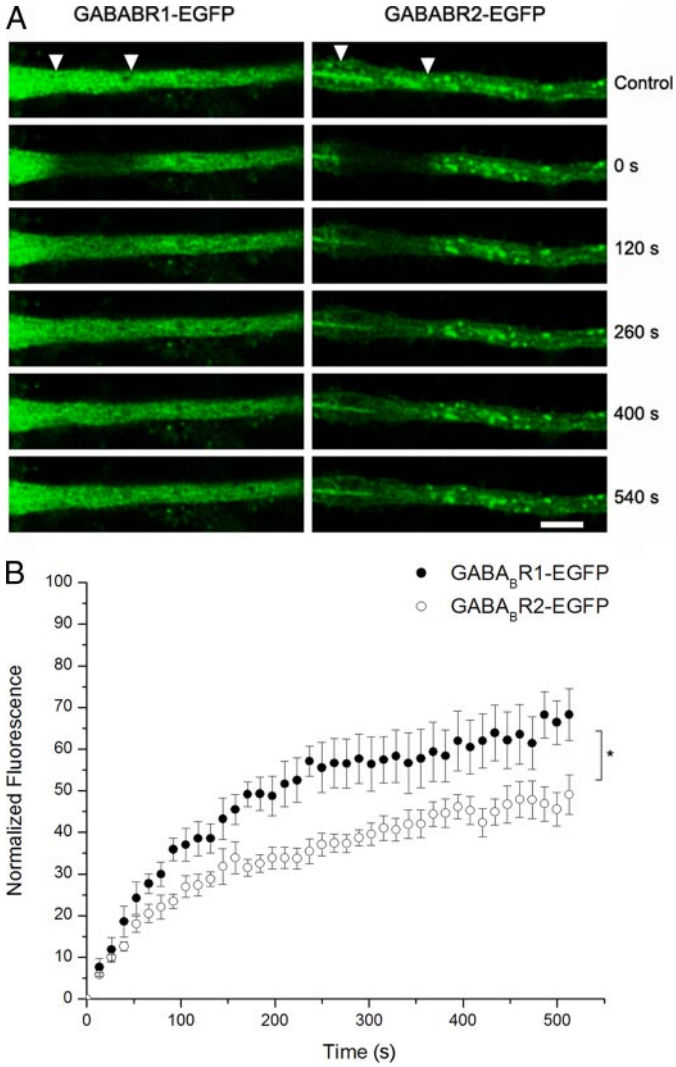

FIGURE 2. **GABA$_B$R1 and GABA$_B$R2 are mobile in dendrites.** *A*, FRAP in 14–16 DIV hippocampal neurons expressing GABA$_B$R1-EGFP or GABA$_B$R2-EGFP. ROIs were placed over experimental dendrites (*arrowheads*) and photobleached, and 40 consecutive frames were acquired over a period of 9 min. Selected frames are shown. *Scale bars*, 10 μm. *B*, values of photobleached/recovered regions were normalized to control images and plotted against time. GABA$_B$R1-EGFP (*filled circles*) and GABA$_B$R2-EGFP (*empty circles*). The data is the average of five to six independent measurements ± S. E. (*, $p < 0.05$).

and displayed an irregular fine punctate pattern (Fig. 2*A*, *left*), consistent with its localization in the ER or ER-Golgi intermediate compartment in the absence of GABA$_B$R2 (11, 21, 31). In contrast, the distribution of GABA$_B$R2-EGFP was more heterogeneous, with larger tubulovesicular structures (Fig. 2*A*, *right*). GABA$_B$R1-EGFP and GABA$_B$R2-EGFP recovered efficiently after photobleaching revealing abundant pools of mobile subunits (Fig. 2*A*). However, the extent of recovery was different for GABA$_B$R1 and GABA$_B$R2. Although GABA$_B$R1 recovered ~70%, GABA$_B$R2 only reached ~50% of the original fluorescence (Fig. 2*B*).

We also performed time-lapse microscopy to explore the mobility of GABA$_B$R subunits using mRFP fused to GABA$_B$R1 and GABA$_B$R2-EGFP (supplemental Fig. S1). Over a period of 30 min the majority of GABA$_B$R1-mRFP- and GABA$_B$R2-EGFP-containing structures moved independently and in bidirectional fashion (supplemental Fig. S2). These results indicate that GABA$_B$R1 and GABA$_B$R2 are transported in dendrites and suggest that they reside in segregated compartments, which move with different kinetics.

Segregated GABA$_B$R1 and GABA$_B$R2 Subunits Are Abundant in the Brain—To determine whether a significant pool of non-assembled GABA$_B$R subunits exist in intracellular compartments of the brain we complemented our analysis with a biochemical approach. We coimmunoprecipitated GABA$_B$R1 and GABA$_B$R2 from two subcellular rat brain fractions enriched in different membranous organelles (P2, a fraction enriched in plasma membrane and P3, a fraction enriched in light intracellular membranes). Calnexin, an ER resident protein, was enriched in P3 confirming the effectiveness of the differential centrifugation procedure (Fig. 3*B*). Although the net amount of GABA$_B$R1 that coimmunoprecipitated with GABA$_B$R2 was similar in P2 and P3, the total subunit abundance was significantly lower in P2 than in P3 (Fig. 3, *A–D*). Thus, the relative abundance of associated subunits was significantly higher in P2 than in P3 (Fig. 3*E*). These observations demonstrate that the proportion of non-associated subunits is higher in intracellular compartments than in the plasma membrane in the brain.

Segregated GABA$_B$R1 and GABA$_B$R2 Subunits Predominate in Dendritic Intracellular Compartments—We then used quantitative colocalization to discriminate between associated and segregated GABA$_B$R1 and GABA$_B$R2 subunits in dendrites of cultured hippocampal neurons. GABA$_B$R subunits were distributed as densely packed granules, with minor differences during neuronal differentiation (Fig. 4*A*). Merged confocal images revealed a high proportion of non-colocalized subunits (Fig. 4*A*). A quantitative analysis yielded low colocalization between GABA$_B$R1 and GABA$_B$R2 for all stages of differentiation (Fig. 4, *C* and *D*: M_1 GABA$_B$R1/R2: 7 days *in vitro* (DIV), 0.291 ± 0.019; 14 DIV, 0.290 ± 0.016; 21 DIV, 0.296 ± 0.017; M_2 GABA$_B$R2/R1: 7 DIV, 0.305 ± 0.024; 14 DIV, 0.256 ± 0.012; 21 DIV, 0.272 ± 0.021; $n = 6$ cells, 5 slices each). These results demonstrate that a high proportion of GABA$_B$R1 and GABA$_B$R2 are segregated in dendrites. Moreover, taking into account that hippocampal neurons actively establish synapses during the first weeks in culture (not shown), they demonstrate that the proportion of subunit association is independent of synaptogenesis. Similar results were obtained in axons (supplemental Fig. S3).

Colocalization was high when a control protein, the GluR2 subunit of the AMPA receptor, was detected with a single primary antibody and two different secondary antibodies, validating the quantitative colocalization method in dendrites (Fig. 4, *B–D*, M_1 GluR2 *green*/*red*: 0.788 ± 0.018; M_2 GluR2 *red*/*green*: 0.785 ± 0.031). In addition, high and almost identical coefficients were obtained when comparing the colocalization of GABA$_B$R1 and GABA$_B$R2 at the plasma membrane of COS-7 cells using antibodies to endogenous C-terminal epitopes or extracellular N-terminal epitope tags (not shown). Furthermore, no antibody-induced clustering was detected (not shown). These results indicate that the antibodies are specific and appropriate for a colocalization analysis and that the analysis is not affected by epitope masking.

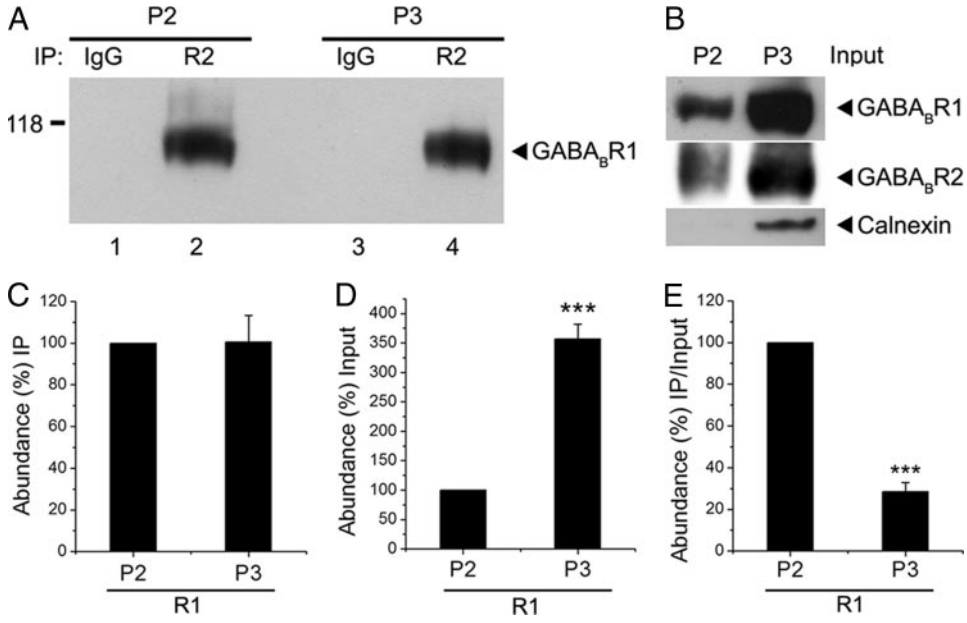

FIGURE 3. **The association of GABA$_B$R1 and GABA$_B$R2 is low in a brain microsomal fraction.** *A*, coimmunoprecipitation of GABA$_B$R1 and GABA$_B$R2 from different membrane preparations. P2 (*lanes 1* and *2*) and P3 fractions (*lanes 3* and *4*) were prepared from adult rat brains. Samples were immunoprecipitated with control IgG (*lanes 1* and *3*) or GABA$_B$R2 antibodies (*lanes 2* and *4*), separated by SDS-PAGE and immunoblotted with GABA$_B$R1 antibodies. *B*, the P2 and P3 fractions prior to immunoprecipitations were used to control the abundance of GABA$_B$R1, GABA$_B$R2, and calnexin. *C*, immunoblots for immunoprecipitations of GABA$_B$R1 from P2 or P3 were analyzed by densitometry and average values ± S.E. were plotted for each fraction ($n = 3$ independent fractionation and immunoprecipitation experiments). *D*, same as above for the total abundance GABA$_B$R1 in each fraction. *E*, values of immunoprecipitations were normalized to the abundance of GABA$_B$R1 in the corresponding fraction and average values ± S.E. were plotted for each fraction (***, $p < 0.001$).

To provide an independent measurement of the proportion of segregated subunits we used recombinant Myc-GABA$_B$R1 and HA-GABA$_B$R2 in hippocampal neurons. Importantly, the distribution patterns of recombinant and endogenous subunits were indistinguishable (Fig. 4, *A* and *E*). By detecting the N-terminal epitope tags under non-permeabilized conditions we had access exclusively to the subunits at the cell surface. Alternatively, by detecting the same epitopes under permeabilized conditions we evaluated the total population of cell surface plus intracellular subunits. As expected, GABA$_B$R1 and GABA$_B$R2 displayed high colocalization at the dendritic plasma membrane (Fig. 4, *E* (*upper panel*) and *G*, M_1 GABA$_B$R1/R2: 0.609 ± 0.014, M_2 GABA$_B$R2/R1: 0.645 ± 0.015, $n = 5$ cells, 5 slices each). In contrast, the colocalization was significantly lower when the intracellular populations were included in the analysis (Fig. 4, *E* (*lower panel*) and *G*, M_1 GABA$_B$R1/R2: 0.355 ± 0.029, M_2 GABA$_B$R2/R1: 0.378 ± 0.034, $n = 5$ cells, 5 slices each). We also analyzed the colocalization between GABA$_B$R1 and a chimera containing the N terminus and seven transmembrane domains of GABA$_B$R2 fused to the C terminus of GABA$_B$R1 (GABA$_B$R2$_{R1C}$), including the ER retention motif (22). Colocalization between this pair was significantly higher than control (Fig. 4, *F* and *G*).

To support these observations we evaluated the intracellular colocalization of endogenous GABA$_B$R subunits. We could not directly monitor the surface/intracellular ratio for native GABA$_B$Rs due to the lack of antibodies against extracellular epitopes. However, we measured the differences between a region "near the plasma membrane" (PM) and the "core region" (CR) of a dendrite. We discriminated between PM and CR through image processing by isolating 0.6-μm strips along the margins of the dendrite. Colocalization was significantly higher for PM than CR (Fig. 4*H*, M_1 GABA$_B$R1/R2: PM, 0.425 ± 0.011; CR, 0.197 ± 0.009, $n = 6$ cells, 5 slices each).

A visual examination also revealed that GABA$_B$R subunits showed little colocalization in the cell body (Fig. 4*I*). Although GABA$_B$R1 was prominent in a ring around the nucleus and displayed a homogeneous pattern in the rest of the soma, GABA$_B$R2 was heterogeneous with abundant staining near the cell surface and in the perinuclear area. Taken together these observations reveal the prevalence of segregated subunits in intracellular compartments of cell bodies and dendrites. They also indicate that the C termini of GABA$_B$R1 and GABA$_B$R2 are essential to keep the subunits segregated in intracellular compartments of dendrites.

Heteromeric Receptors Are Preferentially Associated to the Plasma Membrane, but Disruption of ER Export Results in Intracellular Somatodendritic Accumulation—We took advantage of BiFC to unambiguously localize the assembled heteromer within the neuron. GABA$_B$R1 was fused to YFP-N, whereas GABA$_B$R2 was fused to YFP-C. GABA$_B$R-dependent BiFC signal (GABA$_B$R-BiFC) was only observed when neurons were cotransfected with Myc-GABA$_B$R1-YFP-N and HA-GABA$_B$R2-YFP-C, and not when the constructs were expressed independently (supplemental Fig. S4). GABA$_B$R-BiFC occurred predominantly at the plasma membrane of somatic and dendritic compartments as indicated by the overlap with simultaneous surface staining of GABA$_B$R1 (Fig. 5*A*). Occasionally GABA$_B$R-BiFC accumulated in intracellular compartments where it did not colocalize with the ER or the Golgi apparatus (Fig. 5, *B* and *C*). These observations are in agreement with the lack of subunit colocalization in intracellular compartments of dendrites.

We then used BFA to block the ER to Golgi transport (32). Acute BFA treatment caused the dispersal of the Golgi apparatus but had no effect on GABA$_B$R-BiFC localization (Fig. 6, *A* and *B*). This suggests that the pool of assembled GABA$_B$Rs in transit through the secretory pathway is small compared with the levels of heteromers at plasma membrane at steady state. To capture this limited in-transit pool we incubated neurons for a prolonged period with a low concentration of BFA (33). As expected, the Golgi apparatus was dispersed after BFA treatment, but now the majority of GABA$_B$R-BiFC remained within intracellular compartments in the cell body and dendrites (Fig. 6*C*).

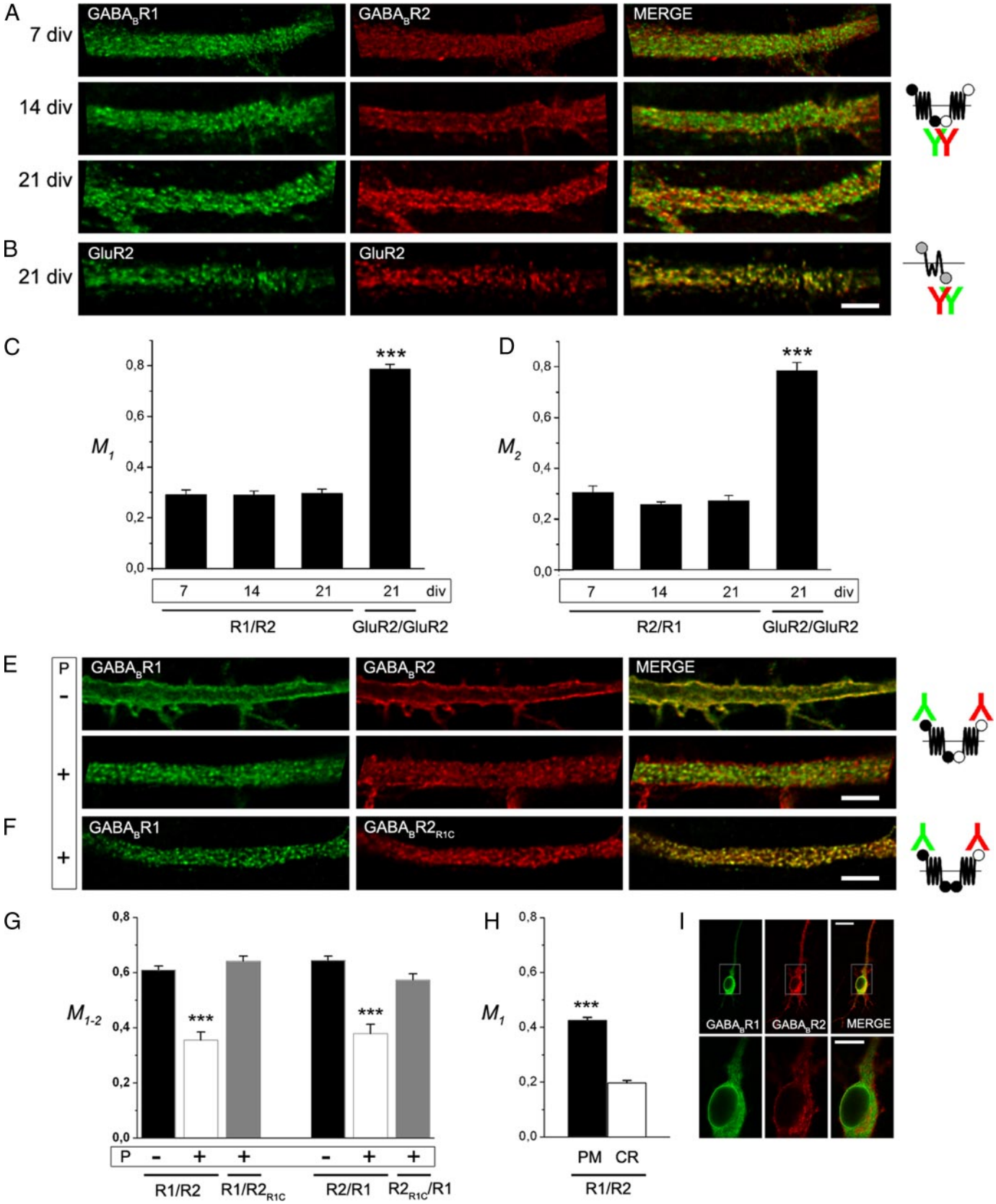

Finally, we expressed GABA$_B$R-BiFC in the presence of Sar1[H79G], a dominant negative form of Sar-1 that is locked in a GTP-bound state and blocks export from the ER (32). Importantly, in the presence of Sar1[H79G] GABA$_B$R-BiFC accumulated intracellularly in the soma and dendrites (Fig. 6*D*). Consistently, the colocalization between GABA$_B$R-BiFC and the ER

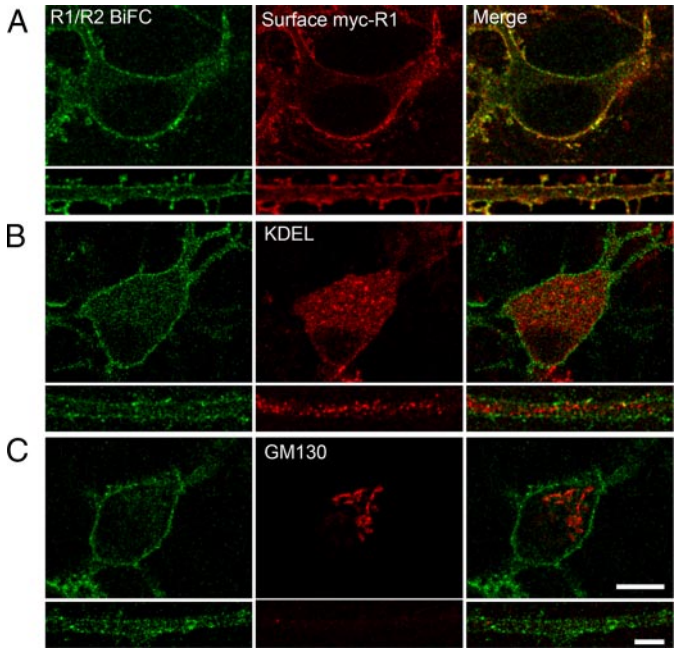

FIGURE 5. **BiFC reveals abundant heteromeric GABA$_B$Rs at the plasma membrane.** *A*, 9–14 DIV rat hippocampal neurons grown in culture were cotransfected with Myc-GABA$_B$R1-YFP-N and HA-GABA$_B$R2-YFP-C. Neurons were fixed and labeled with antibodies to the N-terminal Myc epitope in GABA$_B$R1 to detect surface GABA$_B$Rs (*red*). GABA$_B$R-BiFC was detected without staining (*green*). Merged images are shown on the *right*. *B*, same as above for neurons labeled with anti-KDEL antibodies to detect the ER. *C*, same as above for neurons labeled with anti-GM130 antibodies to detect the Golgi apparatus. Cell bodies are shown on *top* and dendrites *below*. *Scale bars A–C*: somas, 10 μm; dendrites, 5 μm.

was significantly increased in the presence of Sar1[H79G] indicating that GABA$_B$R-BiFC was retained in the ER in dendrites (Fig. 6, *E* and *F*). Taken together these observations strongly support the notion that GABA$_B$R subunits assemble in the ER throughout the somatodendritic compartment.

DISCUSSION

The existence of heteromeric GABA$_B$Rs at the cell surface of neurons has been convincingly demonstrated by biochemical, functional, and microscopic observations (16, 21, 34–37). Likewise, the ER retention of GABA$_B$R1 and the necessary assembly with GABA$_B$R2 have been shown in a variety of cellular contexts (9). However, the relationship between GABA$_B$R trafficking and the geometrical arrangement of the secretory pathway in neurons has received limited attention. Our findings conclusively show that GABA$_B$R subunits are abundant and segregated in intracellular compartments. They provide compelling evidence for the absence of long haul post-Golgi vesicles containing assembled GABA$_B$Rs in dendrites. They do not challenge the functional heteromerization hypothesis. Rather, they suggest that assembly of GABA$_B$R1 and GABA$_B$R2 and export from the ER are processes that occur throughout the somatodendritic compartment.

Combined with previous reports a model emerges to explain the availability of GABA$_B$Rs at the plasma membrane in neurons. First GABA$_B$R subunits are synthesized in the neuronal cell body and move along dendritic ER membranes. Because GABA$_B$R2 progresses freely through the secretory pathway (9) it picks up ER-retained GABA$_B$R1, and the resulting heteromer rapidly exits the ER in the cell body and dendrites. Continuously, the assembly of intracellular subunits contributes to the turnover of the surface receptors. Once at the plasma membrane GABA$_B$Rs are endocytosed as heteromers in a constitutive manner and undergo efficient recycling (38).

The Presence of Segregated Subunits Defines the Mode of Receptor Trafficking—Our results suggest the existence of negative regulatory factors such as chaperones or specialized subdomains of the ER that prevent heteromeric assembly immediately after synthesis in the cell body. The differential distribution of resident proteins in sub-domains of the ER has been reported before. For example calsequestrin, a luminal resident of the ER, distributes differentially depending on its oligomeric state (39). Regarding ER regulatory proteins 14-3-3 and coatomer complex protein I have been proposed to participate in the ER retention of GABA$_B$Rs (31). Several other proteins interact with the receptor subunits throughout the secretory pathway (*e.g.* msec7-1, C/EBP homologous protein, Marlin-1, activating transcription factor 4, and G protein-coupled receptor kinase 4) and may block their association temporarily (40). In addition, the ER retention and trafficking properties of GABA$_B$ receptors are modulated by the distinct class of GABA$_A$ receptors, raising the possibility of physical and functional cross-talk between these ionotropic and metabotropic neurotransmitter receptor systems (41). However, it remains to be established how ER segregation or GABA$_B$R-associated proteins affect trafficking or whether they contribute to regulate the assembly of GABA$_B$Rs. It is also not clear whether recently

FIGURE 4. **GABA$_B$R1 and GABA$_B$R2 are segregated in intracellular compartments of primary dendrites.** *A*, hippocampal neurons were labeled with antibodies to GABA$_B$R1 (*green*) and GABA$_B$R2 (*red*). Images were merged to visualize colocalization in dendrites (*right*). *Drawings* on the *right*: *circles* correspond to native epitopes; *black*, GABA$_B$R1; *empty*, GABA$_B$R2; *red* and *green symbols* correspond to secondary antibodies. *B*, same as above in neurons labeled with primary antibodies to GluR2 and two secondary antibodies. Images were merged to visualize colocalization (*right*). *Drawings* on the *right*: *circles* correspond to native epitopes; *gray*, GluR2; *red* and *green symbols* correspond to secondary antibodies. *Scale bar* for *A* and *B*, 5 μm. *C*, images were processed to quantify colocalization. For GABA$_B$Rs M_1 corresponds to the proportion of GABA$_B$R1, which colocalizes with GABA$_B$R2. For GluR2 M_1 corresponds to the proportion of the *green* fluorophore, which colocalizes with the *red* fluorophore. *D*, for GABA$_B$Rs M_2 corresponds to the proportion of GABA$_B$R2, which colocalizes with GABA$_B$R1. For GluR2 M_2 corresponds to the proportion of the *red* fluorophore, which colocalizes with the *green* fluorophore. Each *bar* is the average of four to six individual neurons containing four to six optical slices each (***, $p < 0.001$). *E* and *F*, 14 DIV hippocampal neurons were transfected with Myc-GABA$_B$R1 and HA-GABA$_B$R2 or with Myc-GABA$_B$R1 and HA-GABA$_B$R2$_{R1C}$. Neurons were fixed, left non-permeabilized ($P-$) or permeabilized ($P+$), and labeled with antibodies to the N-terminal Myc and HA epitopes. *Drawing* on the *right*: *circles* correspond to epitope tags; *black*, GABA$_B$R1; *empty*, GABA$_B$R2; *red* and *green symbols* correspond to secondary antibodies. *Scale bar*, 5 μm. *G*, images were processed to quantify colocalization in dendrites. For GABA$_B$Rs M_1 corresponds to the proportion of GABA$_B$R1, which colocalizes with GABA$_B$R2 or GABA$_B$R2$_{R1C}$ under non-permeabilized (P-) or permeabilized conditions ($p+$). M_2 corresponds to the proportion of GABA$_B$R2 or GABA$_B$R2$_{R1C}$, which colocalizes with GABA$_B$R1. Each *bar* is the average of four to six individual neurons containing four to six optical slices each (***, $p < 0.001$). *H*, 14 DIV hippocampal neurons were labeled as in *A* and processed to quantify colocalization in PM and CR. M_1 corresponds to the proportion of GABA$_B$R1, which colocalizes with GABA$_B$R2. PM: *black bar*, CR: *empty bar*. Each *bar* is the average of six individual neurons containing five optical slices each (***, $p < 0.001$). *I*, same as in *E* showing the somatic region of a permeabilized neuron labeled for Myc-GABA$_B$R1 and HA-GABA$_B$R2. *Lower panels*, high magnification of regions *boxed* above. *Scale bars*: *upper panels*, 20 μm; *lower panels*, 10 μm.

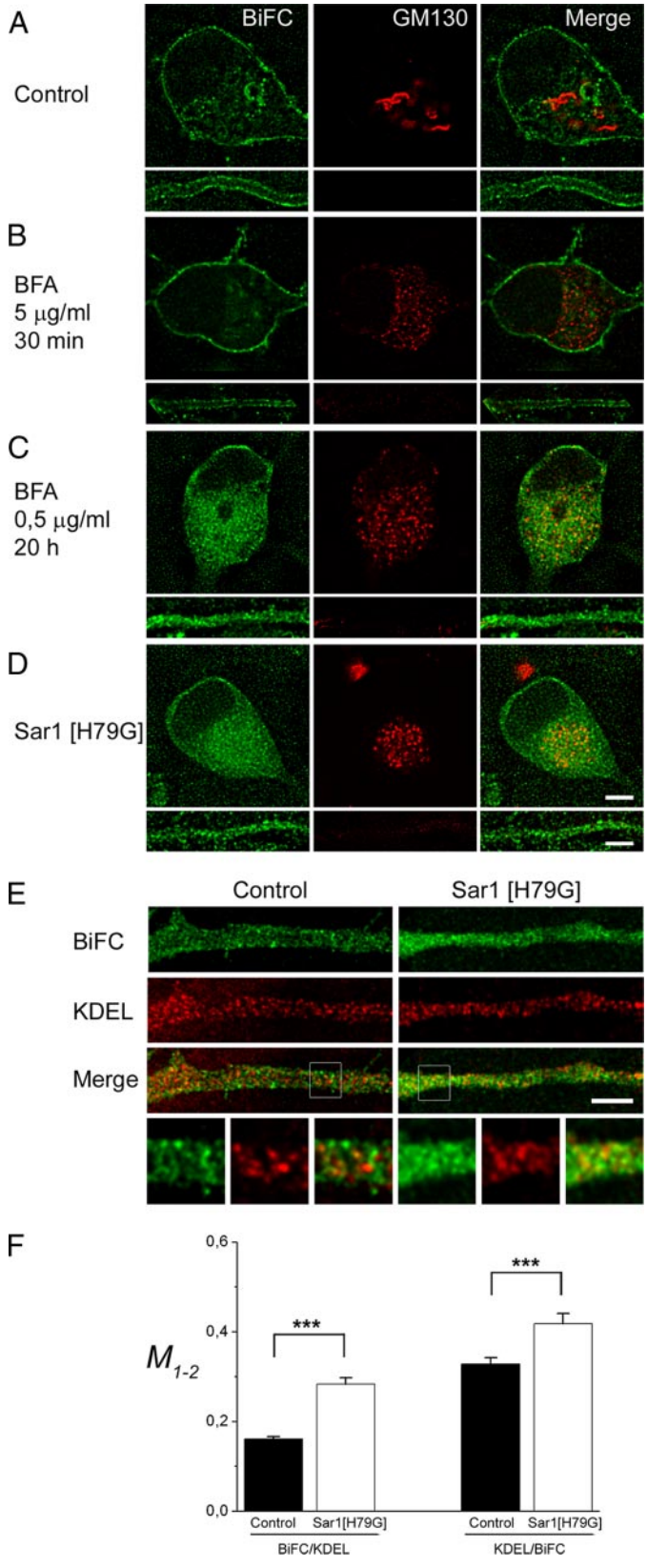

FIGURE 6. **GABA$_B$R1 and GABA$_B$R2 assemble in the soma and dendrites of hippocampal neurons.** *A*, 9–14 DIV hippocampal neurons were cotransfected with Myc-GABA$_B$R1-YFP-N and HA-GABA$_B$R2-YFP-C. Neurons were fixed and labeled with anti-GM130 antibodies to detect the Golgi apparatus (*red*). BiFC fluorescence was detected without staining (*green*). Merged images are shown on the *right*. *B* and *C*, same as above for neurons treated with 5 μg/ml BFA for 30 min or 0.5 μg/ml BFA for 20 h. *D*, 9–14 DIV hippocampal neurons were cotransfected with Myc-GABA$_B$R1-YFP-N, HA-GABA$_B$R2-YFP-C, and Sar-1[H79G]. For each condition somas are shown on *top* and dendrites *below*. *Scale bars A–D*: 5 μm. *E*, 9–14 DIV hippocampal neurons were cotransfected with Myc-GABA$_B$R1-YFP-N and HA-GABA$_B$R2-YFP-C or Myc-GABA$_B$R1-YFP-N and HA-GABA$_B$R2-YFP-C and Sar-1[H79G]. Neurons were fixed and labeled with anti-KDEL to detect the ER. *Scale bars*: *E*, 5 μm; *F*, images from *E* were processed to quantify colocalization. M_1 corresponds to the proportion of GABA$_B$R-BiFC, which colocalizes with KDEL. M_2 corresponds to the proportion of KDEL, which colocalizes with GABA$_B$R-BiFC (control, *black bars*; Sar-1[H79G], *white bars*). Each *bar* is the average of three neurons containing four to six optical slices each (***, $p < 0.001$).

assembled heteromers follow a conventional or a local secretory route after ER export and how ER exit is regulated (42).

Most of the evidence regarding GABA$_B$Rs indicates that the subunits assemble in the ER (9). However, recent reports suggest that GABA$_B$R1 reaches the *cis*-Golgi or the *trans*-Golgi network (31, 36). These observations imply that assembly of the heteromer occurs not in the ER but in a post-ER membrane organelle. Our results are in disagreement with these findings, because upon blockade of ER export assembled GABA$_B$Rs accumulate throughout the somatodendritic ER.

Although electron microscopy studies indicate that GABA$_B$R1 and GABA$_B$R2 localize to similar intracellular membranes in the visual cortex, the degree of intracellular colocalization is lower than at pre- or postsynaptic membranes, supporting our conclusions (43). The differential accumulation of GABA$_B$R subunits in intracellular compartments is not unique and may be common for a variety of multisubunit receptors requiring tight assembly and precise targeting control. For example, the GluR1 and GluR2 subunits of the AMPA receptor accumulate abundantly in intracellular compartments and display significant differences in speed and direction of intracellular mobility (44). In addition, AMPA receptor subunits distribute differentially in intracellular compartments and their distribution coincides with tubulovesicular membranes in the dendritic ER (45). Interestingly, *N*-methyl-D-aspartic acid receptors are also exported from the ER in dendrites (46). Thus, a conserved mechanism may exist to regulate the transport and assembly of receptors through the ER membrane and their assembly en route to the synapse.

Implications for Receptor Availability at the Plasma Membrane—GABA$_B$R-induced currents increase significantly between 5 and 14 DIV in cultured hippocampal neurons (34). Unexpectedly our results demonstrate that the proportion of colocalized GABA$_B$R subunits, an indirect indication of functional receptors, does not change during differentiation. These observations are surprising considering the robust synaptogenic conditions of the culture. Two alternative interpretations of these results are possible. First, the number of associated subunits may increase proportionally to the number of segregated ones. Second, the abundance of membrane receptors may be constant during the initial stages of synaptogenesis, but the gradual acquisition of functional GABA$_B$Rs may be defined by the availability of downstream signaling molecules. Taking into account the continuous increase in the abundance of total GABA$_B$R1 and GABA$_B$R2 during the first 21 DIV, the increase in surface GABA$_B$R2 during the same period, and the constant levels of G-protein inwardly rectifying potassium channel 1 (34), an established downstream signaling molecule for

$GABA_B$Rs, we favor the first alternative and suggest a continual and proportional replenishing of associated $GABA_B$Rs from intracellular segregated pools.

$GABA_B$Rs are also abundant in axons, but their mode of transport remains unexplored (16, 17). Our colocalization analysis also suggests the more controversial mechanism that segregated subunits assemble in axons. This possibility poses additional challenges: although the existence of the ER in axons has been reported (47), the presence of late secretory components is less clear. Therefore, understanding the precise assembly mechanism of $GABA_B$Rs and other multisubunit receptors in axons requires a detailed characterization of the complex morpho-topological distribution of secretory organelles in neurons (48).

Acknowledgments—We thank C. Morales, M. Calegaro, and L. Sandoval for technical assistance and A. Buonanno for carefully reading the manuscript.

REFERENCES

1. Collingridge, G. L., Isaac, J. T., and Wang, Y. T. (2004) *Nat. Rev. Neurosci.* **5,** 952–962
2. Kennedy, M. J., and Ehlers, M. D. (2006) *Annu. Rev. Neurosci.* **29,** 325–362
3. Inoue, A., and Okabe, S. (2003) *Curr. Opin. Neurobiol.* **13,** 332–340
4. Moss, S. J., and Smart, T. G. (2001) *Nat. Rev. Neurosci.* **2,** 240–250
5. Clem, R. L., and Barth, A. (2006) *Neuron* **49,** 663–670
6. Couve, A., Calver, A. R., Fairfax, B., Moss, S. J., and Pangalos, M. N. (2004) *Biochem. Pharmacol.* **68,** 1527–1536
7. Pin, J. P., Kniazeff, J., Binet, V., Liu, J., Maurel, D., Galvez, T., Duthey, B., Havlickova, M., Blahos, J., Prezeau, L., and Rondard, P. (2004) *Biochem. Pharmacol.* **68,** 1565–1572
8. Sakaba, T., and Neher, E. (2003) *Nature* **424,** 775–778
9. Bettler, B., Kaupmann, K., Mosbacher, J., and Gassmann, M. (2004) *Physiol. Rev.* **84,** 835–867
10. Cousins, M. S., Roberts, D. C., and de Wit, H. (2002) *Drug Alcohol Depend.* **65,** 209–220
11. Couve, A., Filippov, A. K., Connolly, C. N., Bettler, B., Brown, D. A., and Moss, S. J. (1998) *J. Biol. Chem.* **273,** 26361–26367
12. Margeta-Mitrovic, M., Jan, Y. N., and Jan, L. Y. (2000) *Neuron* **27,** 97–106
13. Kaupmann, K., Malitschek, B., Schuler, V., Heid, J., Froestl, W., Beck, P., Mosbacher, J., Bischoff, S., Kulik, A., Shigemoto, R., Karschin, A., and Bettler, B. (1998) *Nature* **396,** 683–687
14. Robbins, M. J., Calver, A. R., Filippov, A. K., Hirst, W. D., Russell, R. B., Wood, M. D., Nasir, S., Couve, A., Brown, D. A., Moss, S. J., and Pangalos, M. N. (2001) *J. Neurosci.* **21,** 8043–8052
15. Duthey, B., Caudron, S., Perroy, J., Bettler, B., Fagni, L., Pin, J. P., and Prezeau, L. (2002) *J. Biol. Chem.* **277,** 3236–3241
16. Vigot, R., Barbieri, S., Brauner-Osborne, H., Turecek, R., Shigemoto, R., Zhang, Y. P., Lujan, R., Jacobson, L. H., Biermann, B., Fritschy, J. M., Vacher, C. M., Muller, M., Sansig, G., Guetg, N., Cryan, J. F., Kaupmann, K., Gassmann, M., Oertner, T. G., and Bettler, B. (2006) *Neuron* **50,** 589–601
17. Kulik, A., Vida, I., Lujan, R., Haas, C. A., Lopez-Bendito, G., Shigemoto, R., and Frotscher, M. (2003) *J. Neurosci.* **23,** 11026–11035
18. Kerppola, T. K. (2008) *Annu. Rev. Biophys.* **37,** 465–487
19. Goslin, K., and Banker, G. (1991) in *Culturing Nerve Cells* (Banker, G., and Goslin, K., eds) pp. 251–281, Massachusetts Institute of Technology, Cambridge, MA
20. Jiang, M., and Chen, G. (2006) *Nat. Protoc.* **1,** 695–700
21. Restituito, S., Couve, A., Bawagan, H., Jourdain, S., Pangalos, M. N., Calver, A. R., Freeman, K. B., and Moss, S. J. (2005) *Mol. Cell. Neurosci.* **28,** 747–756
22. Calver, A. R., Robbins, M. J., Cosio, C., Rice, S.Q., Babbs, A. J., Hirst, W. D., Boyfield, I., Wood, M. D., Russell, R. B., Price, G. W., Couve, A., Moss, S. J., and Pangalos, M. N. (2001) *J. Neurosci.* **21,** 1203–1210
23. Couve, A., Thomas, P., Calver, A. R., Hirst, W. D., Pangalos, M. N., Walsh, F. S., Smart, T. G., and Moss, S. J. (2002) *Nat. Neurosci.* **5,** 415–424
24. Kuramoto, N., Wilkins, M. E., Fairfax, B. P., Revilla-Sanchez, R., Terunuma, M., Tamaki, K., Iemata, M., Warren, N., Couve, A., Calver, A., Horvath, Z., Freeman, K., Carling, D., Huang, L., Gonzales, C., Cooper, E., Smart, T. G., Pangalos, M. N., and Moss, S. J. (2007) *Neuron* **53,** 233–247
25. Vidal, R. L., Ramírez, O. A., Sandoval, L., Koenig-Robert, R., Härtel, S., and Couve, A. (2007) *Mol. Cell. Neurosci.* **35,** 501–512
26. Couve, A., Kittler, J. T., Uren, J. M., Calver, A. R., Pangalos, M. N., Walsh, F. S., and Moss, S. J. (2001) *Mol. Cell. Neurosci.* **17,** 317–328
27. Blichenberg, A., Schwanke, B., Rehbein, M., Garner, C. C., Richter, D., and Kindler, S. (1999) *J. Neurosci.* **19,** 8818–8829
28. Costes, S. V., Daelemans, D., Cho, E. H., Dobbin, Z., Pavlakis, G., and Lockett, S. *Biophys. J.* **86,** 3993–4003
29. Espinosa, A., García, A., Härtel, S., Hidalgo, C., and Jaimovich, E. (2008) *J. Biol. Chem.* **284,** 2568–2575
30. Towers, S., Princivalle, A., Billinton, A., Edmunds, M., Bettler, B., Urban, L., Castro-Lopes, J., and Bowery, N. G. (2000) *Eur. J. Neurosci.* **12,** 3201–3210
31. Brock, C., Boudier, L., Maurel, D., Blahos, J., and Pin, J. P. (2005) *Mol. Biol. Cell* **16,** 5572–5578
32. Ward, T. H., Polishchuk, R. S., Caplan, S., Hirschberg, K., and Lippincott-Schwartz, J. (2001) *J. Cell Biol.* **155,** 557–570
33. Seguchi, T., Goto, Y., Ono, M., Fujiwara, T., Shimada, T., Kung, H. F., Nishioka, M., Ikehara, Y., and Kuwano, M. (1992) *J. Biol. Chem.* **267,** 11626–11630
34. Correa, S. A., Munton, R., Nishimune, A., Fitzjohn, S., and Henley, J. M. (2004) *Neuropharmacology* **47,** 475–484
35. Fairfax, B. P., Pitcher, J. A., Scott, M. G., Calver, A. R., Pangalos, M. N., Moss, S. J., and Couve, A. (2004) *J. Biol. Chem.* **279,** 12565–12573
36. Villemure, J. F., Adam, L., Bevan, N. J., Gearing, K., Chenier, S., and Bouvier, M. (2005) *Biochem. J.* **388,** 47–55
37. Filippov, A. K., Couve, A., Pangalos, M. N., Walsh, F. S., Brown, D. A., and Moss, S. J. (2000) *J. Neurosci.* **20,** 2867–2874
38. Vargas, K. J., Terunuma, M., Tello, J. A., Pangalos, M. N., Moss, S. J., and Couve, A. (2008) *J. Biol. Chem.* **283,** 24641–24648
39. Gatti, G., Trifari, S., Mesaeli, N., Parker, J. M., Michalak, M., and Meldolesi, J. (2001) *J. Cell Biol.* **154,** 525–534
40. Bettler, B., and Tiao, J. Y. (2006) *Pharmacol. Ther.* **110,** 533–543
41. Balasubramanian, S., Teissére, J. A., Raju, D. V., and Hall, R. A. (2004) *J. Biol. Chem.* **279,** 18840–18850
42. Horton, A. C., and Ehlers, M. D. (2003) *J. Neurosci.* **23,** 6188–6199
43. Gonchar, Y., Pang, L., Malitschek, B., Bettler, B., and Burkhalter, A. (2001) *J. Comp. Neurol.* **431,** 182–197
44. Perestenko, P. V., and Henley, J. M. (2003) *J. Biol. Chem.* **278,** 43525–43532
45. Rubio, M. E., and Wenthold, R. J. (1999) *J. Neurosci.* **19,** 5549–5562
46. Aridor, M., Guzik, A. K., Bielli, A., and Fish, K. N. (2004) *J. Neurosci.* **24,** 3770–3776
47. Petersen, O. H., Tepikin, A., and Park, M. K. (2001) *Trends Neurosci.* **24,** 271–276
48. Hanus, C., and Ehlers, M. D. (2008) *Traffic* **9,** 1437–1445